

# Positioning Analysis of HF Monopole Antennas on a Frigate

F. C. S. Assumpção<sup>1</sup> , M. H. C. Dias<sup>2</sup> 

<sup>1</sup>Electrical Engineering Section, Instituto de Engenharia Militar – IME, Praça General Tibúrcio, 80, Urca, 22290-270, Rio de Janeiro, RJ, Brazil, [fca1y2@gmail.com](mailto:fca1y2@gmail.com)

<sup>2</sup>Centro Federal de Educação Tecnológica Celso Suckow da Fonseca – CEFET/RJ, Av. Maracanã, 229, Maracanã, 20271-110, Rio de Janeiro, RJ, Brazil, [mauricio.dias@cefet-rj.br](mailto:mauricio.dias@cefet-rj.br)

**Abstract**— For vehicle tactical radio communications, positioning antennas along the structure is a complex task. In vessels, there are several radio systems installed operating from HF to SHF. Consequently, the antennas need to share the same restricted space while preserving electromagnetic compatibility. In this context, this work presents a parametric analysis of the positioning of HF monopole antennas on the upper bridge of a typical Navy frigate. A numerical antenna analysis tool was chosen to support the intended analysis. Six positioning scenarios were simulated, evaluating the performance change of figures of merit such as the reflection coefficient and gain, due to the mutual coupling between the antennas and the main metallic objects within their close range. Furthermore, from the analysis, it was possible to establish recommended distances of decorrelation between the antenna and the main nearby objects.

**Index Terms**— HF antennas, monopole antennas, mutual coupling, naval communications.

## I. INTRODUCTION

The relative positioning of an antenna in vehicles, aircraft, or vessels for tactical applications is a complex task [1], [2], as highlighted by several factors in [3]–[7]. The mutual coupling between the antenna and the conducting elements in the vicinity, the finite and irregular dimensions of the ground plane [8], aspects of electromagnetic compatibility [9], [10], among others, are some examples of these critical issues.

In the context of radio communications systems operation in ships, there are some works that discuss the antenna positioning, as in [11]–[17], all of them addressing HF antennas. Furthermore, these works address antenna projects using part of the ship's structure (mast or chimney) to compose the radiant elements. In [18], an analysis of the electromagnetic compatibility and interference of HF antennas in ships is discussed.

Considering a frigate, as an example, the antenna positioning complexity is high due to dozens of radio communications systems, operating in bands from HF to UHF, each with their respective antenna. In particular, HF antennas, usually monopoles [19], are typically installed either at the chimney surroundings or on the upper bridge (the name used for the highest deck of the vessel, in the naval context).

Only after satisfying tests for all systems, including the radio communications systems, it is possible to commission a Navy ship. It is understandable, therefore, that adequate theoretical and practical

knowledge is required in any antenna positioning work in such scope. However, as far as the bibliographical review of this work has reached, the problem of evaluating the antenna positioning in naval vessels seldom is straightforwardly addressed in the pertinent literature.

Thus, the purpose of this work is to present a parametric analysis of HF monopole antennas positioning on the upper bridge of a typical Navy frigate. This analysis was performed based on numerical simulations, using antenna analysis software, and incorporating to the simulated model only the main elements of the scenario, besides the antennas. Both radiation pattern and circuit element behavior were analyzed accordingly to the positioning parameters in the upper bridge scenario.

Section II presents the methodology of this work. Section III describes the simulations settings. The intended analysis is discussed in Section IV. Section V concludes the work.

## II. METHODOLOGY

In frigates, usually the spot where there is the greatest concentration of HF antennas is the upper bridge, which is very close to the main mast, as exemplified by Fig. 1a. Therefore, such scenario was chosen as the most representative for the intended numerical analysis.

The electromagnetic coupling was assessed mainly regarding the effects of the main mast and of the proximity of the antenna to the upper bridge edges. The coupling between a pair of close monopoles was also analyzed. To achieve the proposed objectives, a parametric analysis of a simplified version of the chosen scenario was conceived. The idea was to perform parametric sweeps varying a few geometrical parameters, in order to identify those that led to more significant changes in the antenna behavior, in comparison to the reference case of a monopole in free space over an ideal infinite perfect electrical conductor (PEC) ground plane. Among the several tools that implement numerical methods for antenna analysis [20], CST Studio Suite® [21] was chosen in this work. Fig. 1b illustrates the chosen scenario modeled in CST. All elements, antennas, mast and upper bridge, were modeled as PEC. The ( $z = 0$ ) plane was also modeled as an infinite PEC ground.

Two distinct quarter-wavelength ( $\lambda/4$ ) wire monopoles were chosen to represent the HF antennas in this work, with  $\lambda = 44$  and 20 m. In frigates, it is usual to have 11-m monopoles, that would present first resonance at 6.81 MHz, justifying the first choice. The second, a 5-m monopole, has its first resonance at 15 MHz, representing an alternate choice of antenna for use at the mid-range HF band. In both cases, the wire radius was equal to 2.5 mm.

The antenna behavior was analyzed by means of a few figures of merit, namely the reflection coefficient,  $S_{11}$  (for a reference impedance of 50  $\Omega$ ), the input impedance, and the gain pattern. The mutual coupling between a pair of monopoles was evaluated by the transmission coefficient between them,  $S_{21}$  (also for a reference impedance of 50  $\Omega$ ). The circuit parameters were observed within frequency ranges close to those expected resonances (6.81 and 15 MHz), while the gain patterns were analyzed at the simulated resonances of 6.57 and 14.61 MHz, for the antennas with  $\lambda = 44$  and 20 m, respectively.

Thus, to understand how the structure impacts the antenna performance, data from simulations with and without the mast were compared. To verify the effect of the antenna positioning on the ground plane (structure), data obtained in the simulations in several positions without the mast were compared with those obtained for the reference case. Furthermore, in order to verify how the mast and the edge proximity affected the key figures of merit, data from simulations with the mast were compared

with those without it. Finally, the coupling between antennas was assessed by simulating the scenario of interest with the same conditions adding one more antenna, with and without the mast, using as further references the simulations with only one antenna. It is worth mentioning that, before running all simulations and generating the intended results, a convergence analysis was carried out in CST, to establish the accuracy and the meshing strategy of the time domain solver that would be adequate enough. In order to do that, the scenario with more elements was considered.

From the simulated results, a few decorrelation distances were also estimated, in order to help those in charge of the task of positioning HF monopoles on an upper bridge. The meaning of decorrelation here is that the effects of mutual coupling and other deviations regarding the reference case may be considered negligible. Therefore, a pair of such distances from the antenna to the mast were identified, as well as the distance between a pair of monopoles.

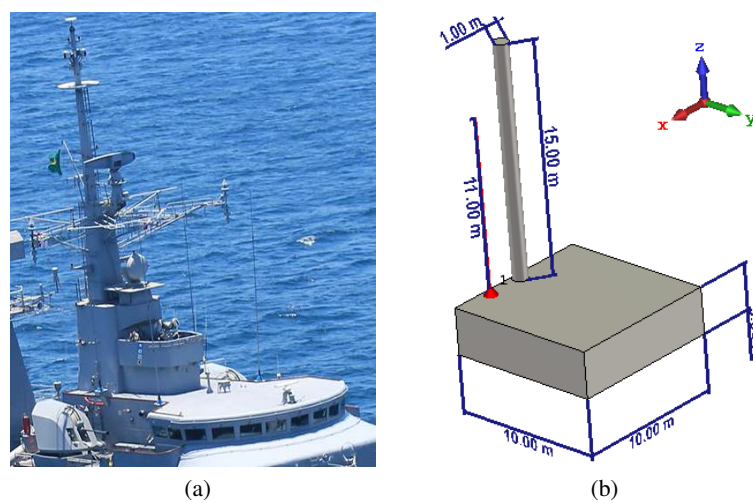


Fig. 1. Upper bridge of a typical frigate. a) Snapshot of an actual upper bridge, b) Simplified model used in simulations.

### III. SIMULATIONS SETTINGS

In all settings, the monopoles were parallel to the  $z$ -axis, as well as the mast, as illustrated in Fig. 1b.

#### A. Simulations T1 and T2

These simulations were conceived to evaluate the effects of a metallic obstacle (the mast) and the antenna's proximity to the upper bridge edges. In simulation T1, the distance between the antenna and the upper bridge edge closest to the mast,  $d_y$  (see Fig. 2a), was fixed and equal to 0.5 m. The antenna positioning relative to the mast was varied along the  $x$ -axis only. Thus, the distance  $d_{am}$  varied from 0.2 to 4.5 m, in steps of 0.4 m, see Fig. 2a. Simulation T2 has the same configuration, but without the mast. The  $d_{am}$  span corresponded to a relative variation of 0.004 to 0.1  $\lambda$  for the antenna with  $\lambda = 44$  m, and 0.01 to 0.225  $\lambda$  for the antenna with  $\lambda = 20$  m.

#### B. Simulations T3 and T4

These simulations were similar to the previous ones. Instead of varying the distance between the antenna and the mast along the  $x$ -axis, the parameter sweep was along the  $y$ -axis here. Thus, in

simulation T3, the antenna was positioned at  $d_{am} = 3$  m (based on results from the previous simulations) and the distance  $d_y$  was varied from 1 to 9 m, in steps of 2 m. The situations in which the antenna was on either edges,  $d_y = 0$  or 10 m, see Fig. 2a, were also considered. Simulation T4 had the same configuration, but without the mast. The  $d_y$  span corresponded to a relative variation of 0.02 to 0.23  $\lambda$  for the antenna with  $\lambda = 44$  m, and 0.05 to 0.5  $\lambda$  for the antenna with  $\lambda = 20$  m. It is worth remarking that, typically, in frigates, the zone corresponding to  $d_y > 7.5$  m on the upper bridge is restricted for antenna positioning, due to the presence of other objects required for the vessel operation.

### C. Simulations T5 and T6

These simulations were conceived to investigate the effects of the electromagnetic coupling between a pair of parallel monopoles, in addition to the aspects already considered in the previous simulations. Thus, another geometrical parameter was introduced, the distance between the monopoles,  $d_{a12}$ , which was varied from 1 to 7 m, in steps of 1 m, see Fig. 2b. The  $d_{a12}$  span corresponded to a relative variation of 0.02 to 0.16  $\lambda$  for the antenna with  $\lambda = 44$  m, and 0.05 to 0.35  $\lambda$  for the antenna with  $\lambda = 20$  m. Based on the results of the previous simulations, the antennas were positioned as follows. Antenna 1 (A1) position was varied along the  $y$ -axis, changing  $d_{a12}$  while  $d_{am}$  was kept fixed at 3 m. Antenna 2 (A2) was kept fixed, with its  $d_{am} = 3$  m and its  $d_y = 7.5$  m, as depicted in Fig. 2b. Simulation T6 had the same configuration, but without the mast.

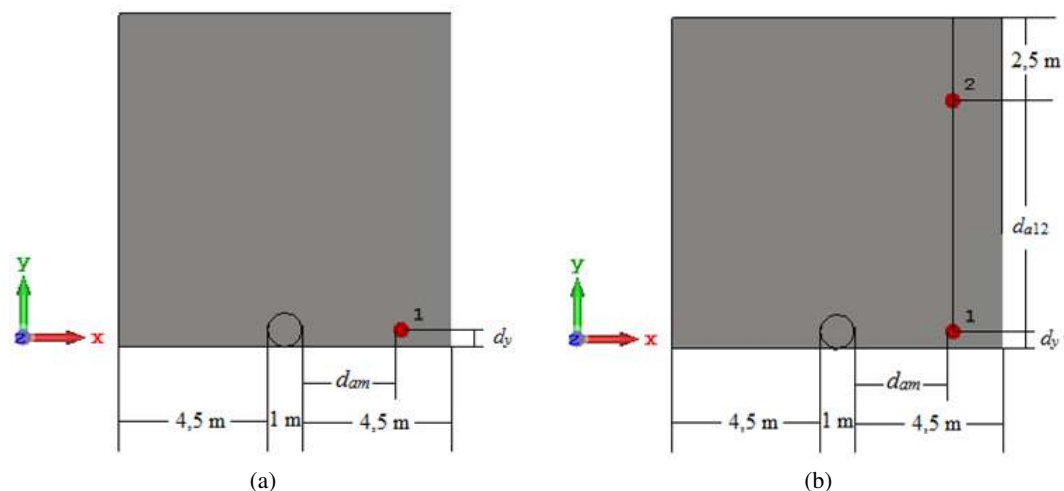


Fig. 2. Main geometrical parameters considered in the analysis. a) Simulations T1, T2, T3 and T4, b) Simulations T5 and T6.

## IV. ANALYSIS

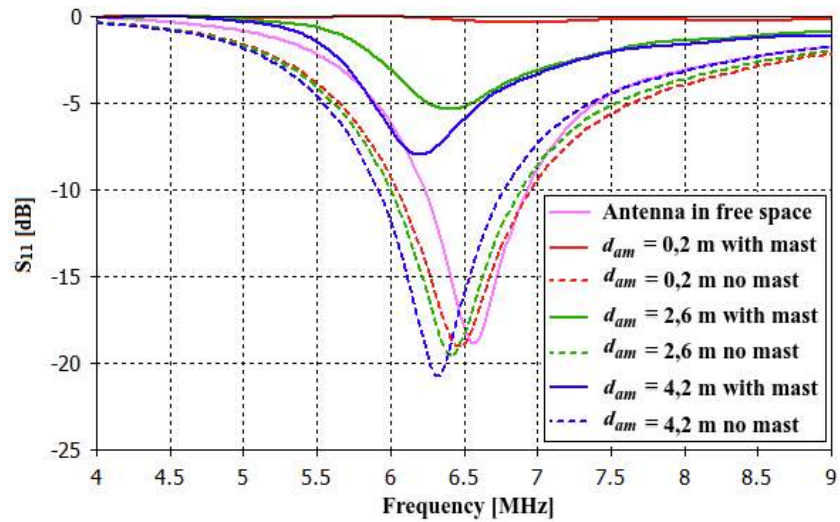
### A. Simulations T1 to T4

The reflection coefficient frequency responses are shown in Fig. 3. As it can be noticed, different responses are achieved as the antenna is repositioned along the  $x$ -axis. The performance also differs from the one obtained for the reference ideal case ( $\lambda/4$  monopole antenna over the infinite PEC ground plane). Thus, it turns out that, as the antenna approaches the upper bridge edge, the resonance frequency and the  $S_{11}$  values decrease slightly for the two scenarios (with or without the mast) and the two different antenna lengths.

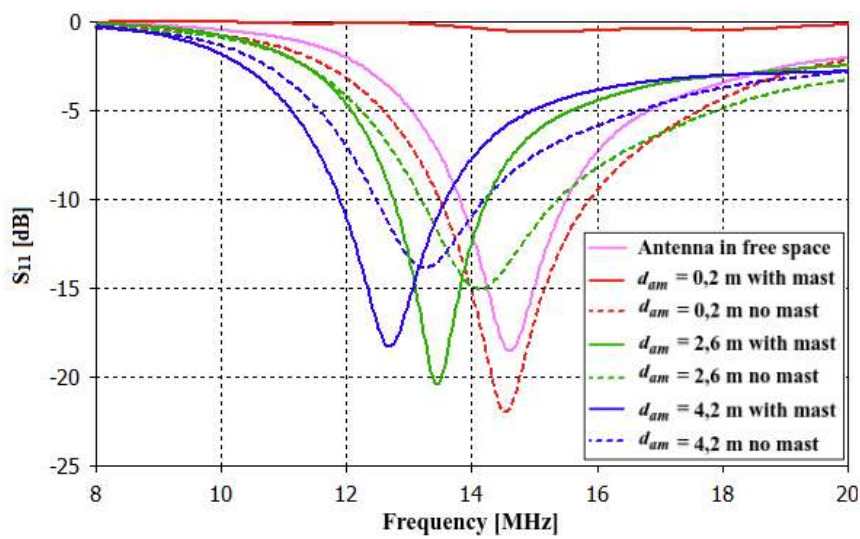
For the antenna with  $\lambda = 44$  m, see Fig. 3a, without the mast, among the various positions, the resonance frequency varies up to 0.2 MHz, and the maximum variation to the reference is 4.56%. The minimum value of the reflection coefficient varies up to 2.6 dB for the various positions, and the maximum difference of this value, concerning the reference, is equal to 2.7 dB. When considering the mast in the simulation scenario, the resonance frequency also undergoes small changes, increasing its variation to the reference to 6.4%. On the other hand, the significant degradation of the coefficient of reflection is noteworthy. The variation of the minimum values of the reflection coefficient for the several positions increases from 2.6 to 8 dB, and the least difference of this value to the reference is 10.6 dB.

As for the antenna with  $\lambda = 20$  m, see Fig. 3b, the resonance frequency behaves similarly to the larger antenna. However, it shows a variation that is greater than that of the reference (9 and 17%, for the scenarios without and with the mast, respectively). The minimum value of the reflection coefficient behaves differently relative to the larger antenna. Without the mast, it increases smoothly as the antenna approaches the upper bridge edge. On the other hand, with the mast, the reflection coefficient rapidly decreases as the antenna position gets farther from the mast and approaches the upper bridge edge. This behavior goes up to  $d_{am} = 3$  m, then  $S_{11}$  starts to increase. The mast degrades the reflection coefficient up to 21.4 dB. The coupling between the antenna and the mast is significant up to  $d_{am} = 2.3$  m. From that distance on, the reflection coefficient performs almost the same way in both cases, with or without the mast. Moreover, the variation of the reflection coefficient is greater when the mast is considered.

The input resistance and reactance in different positions are represented, respectively, in Fig. 4 and Fig. 5, where it is possible to observe that, in the scenario without the mast, for the antenna with  $\lambda = 44$  m, and for the different positions, there is a small variation of such parameters up to the resonance frequency. After this frequency, the variation of these parameters as the antenna gets closer to the edge is more pronounced. As for the antenna with  $\lambda = 20$  m, the variations are greater over the entire observation range. It is also possible to observe that the input resistance is greater than the reference over the whole frequency range. When analyzing the simulations with the mast, the variations of these parameters with the positioning are more significant, mainly from the resonance frequency on. The input resistance is smaller than the one in the scenario without the mast in the whole band, for the antenna with  $\lambda = 44$  m. It is also noticeable that, as the antenna gets farther from the mast, the input resistance increases. The variations observed in these parameters for the antenna with  $\lambda = 20$  m are greater, indicating that it is more susceptible to the coupling effects caused by both the edge and the mast.

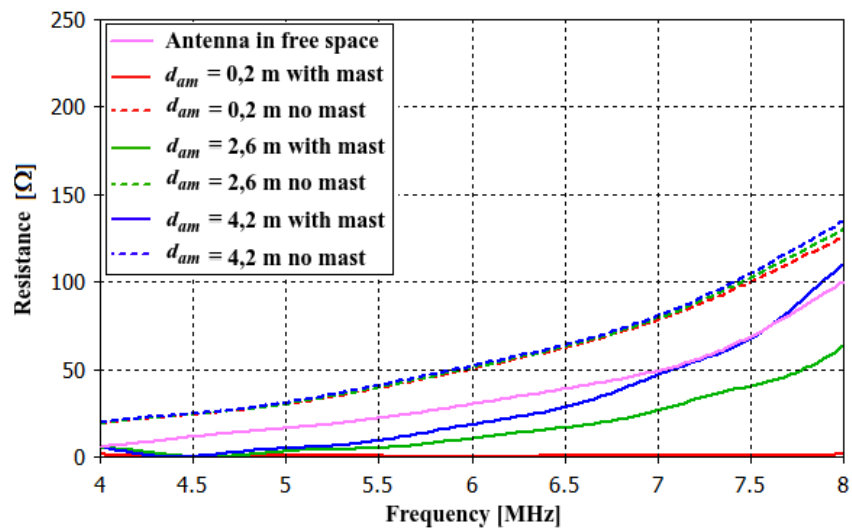


(a)

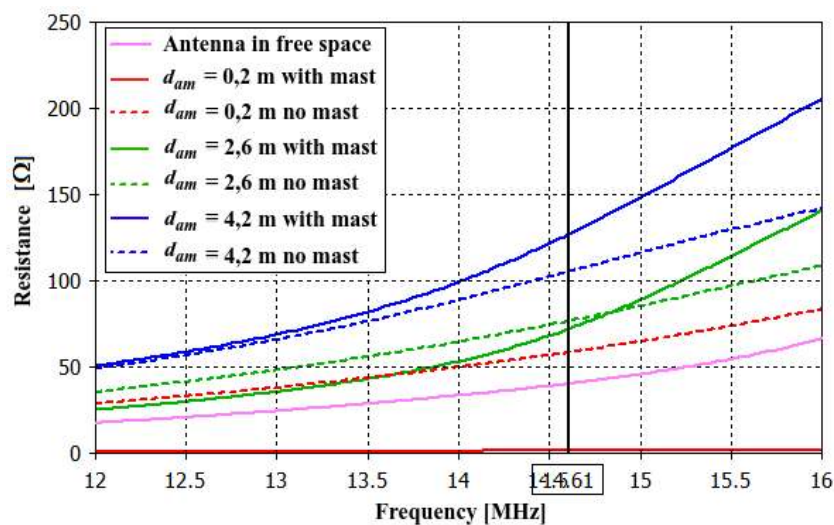


(b)

Fig. 3. Reflection coefficient for simulations T1 and T2. a) Antenna with  $\lambda = 44$  m, b) Antenna with  $\lambda = 20$  m.

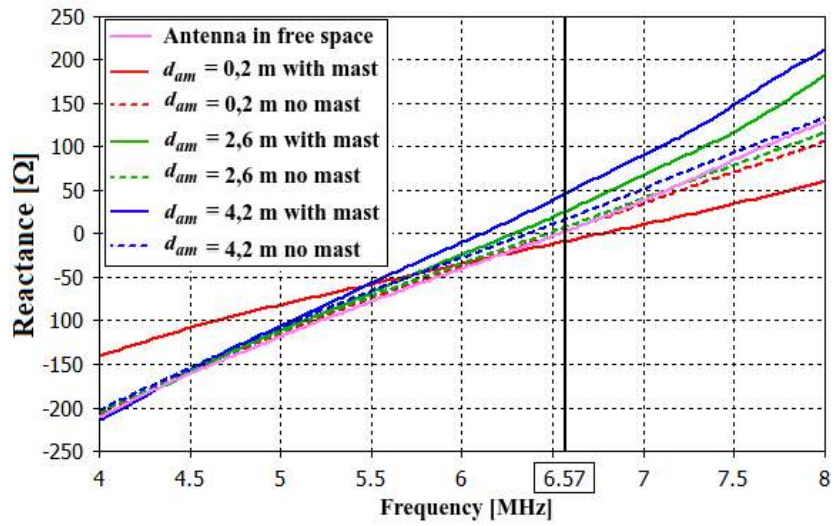


(a)

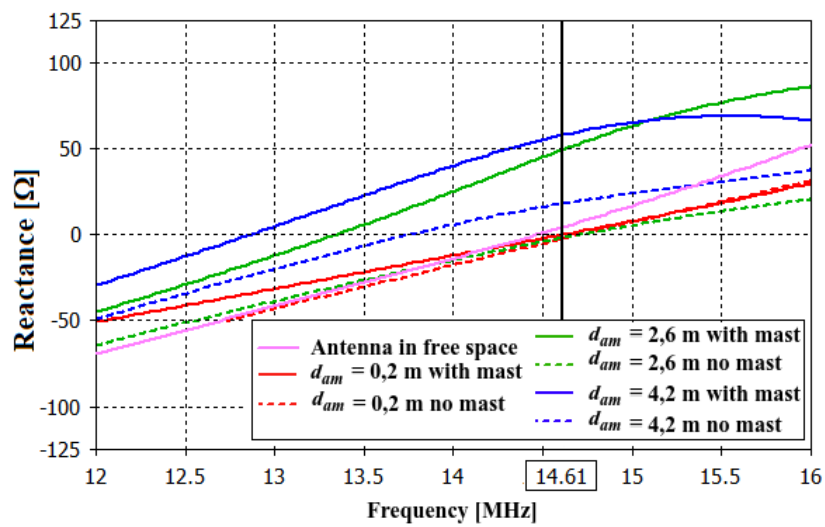


(b)

Fig. 4. Resistance for simulations T1 and T2. a) Antenna with  $\lambda = 44$  m, b) Antenna with  $\lambda = 20$  m.



(a)



(b)

Fig. 5. Reactance for simulations T1 and T2. a) Antenna with  $\lambda = 44$  m, b) Antenna with  $\lambda = 20$  m.



Regarding the gain radiation pattern, in the  $\phi = 0^\circ$  plane, see Fig. 6, without the mast, when varying the antenna positioning along the  $x$ -axis ( $\phi = 0^\circ$ ), as it approaches the edge of the ground plane, the main lobe points to  $\phi = 180^\circ$ , direction where the ground plane portion seen by the antenna is the largest. This behavior is expected, according to the analysis presented in [22]. For the antenna with  $\lambda = 44$  m, the gain in  $\theta = 0^\circ$  increases as the antenna approaches the edge, but it is at least 15 dB less than the main lobe gain. In the scenario with the mast, the pattern changes considerably, with the main lobe pointing to  $\phi = 0^\circ$ , and the maximum gain increases as the antenna gets farther away from the mast. For the antenna with  $\lambda = 20$  m, the  $\phi = 0$  plane gain pattern behaves similarly, but the gain in  $\theta = 0^\circ$  is greater, being at least 8 dB less than the main lobe gain.

In the  $\phi = 90^\circ$  ( $yz$ ) plane, perpendicular to the plane in which the antenna position is varied ( $xz$ ), the performance was not significantly affected neither by the presence of mast, nor by the variation of  $d_{am}$ , for both antenna lengths.

Finally, in the  $\theta = 90^\circ$  plane, see Fig. 7, without the mast, there is a slight loss of the circular shape of the gain pattern due to the proximity of the edge, behavior foresaw in [22]. With the mast, the gain pattern becomes directive, and as  $d_{am}$  increases, the maximum gain increases as well, and the angle of maximum radiation decreases, see Fig. 8.

For simulations T3 and T4, in which  $d_{am} = 3$  and  $d_y$  was varied, it was observed that the mast influence is not significant, for both antenna lengths. The performances regarding the impedance and gain pattern were analogous to the ones observed in simulations T1 and T2. Nonetheless, from these results, it was possible to estimate proper decorrelation distances, as discussed ahead.

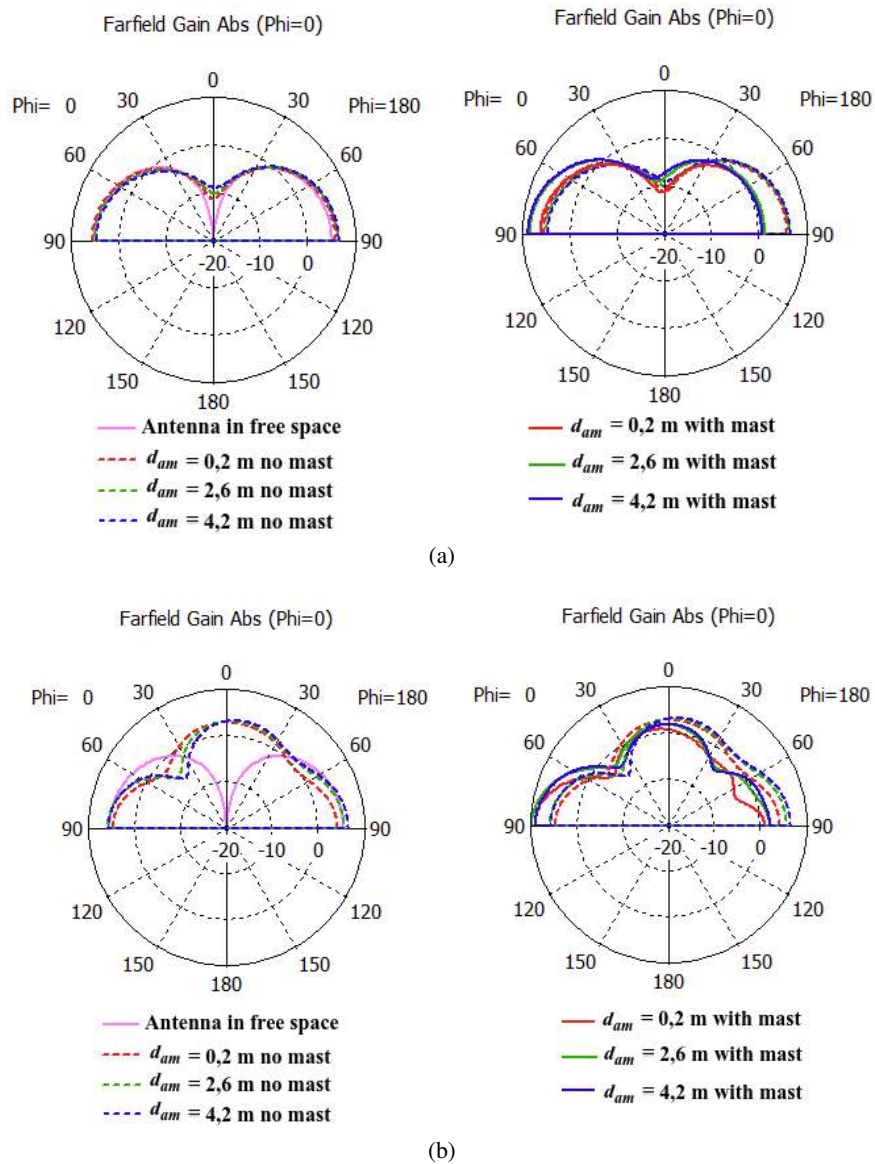


Fig. 6. Gain pattern in the  $\phi = 0^\circ$  plane, in the resonance frequency, for simulations T1 and T2. a) Antenna with  $\lambda = 44$  m, b) Antenna with  $\lambda = 20$  m.

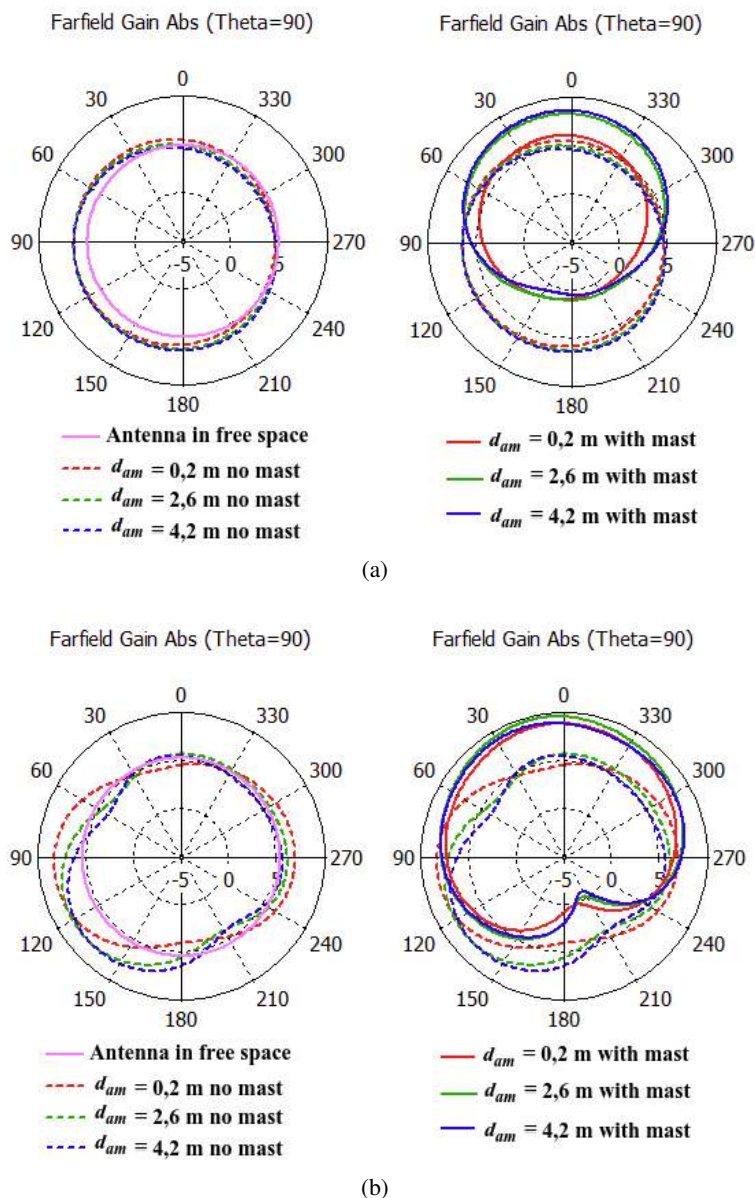


Fig. 7. Gain pattern in the  $\theta = 90^\circ$  plane, in the resonance frequency, for simulations T1 and T2. a) Antenna with  $\lambda = 44$  m, b) Antenna with  $\lambda = 20$  m.

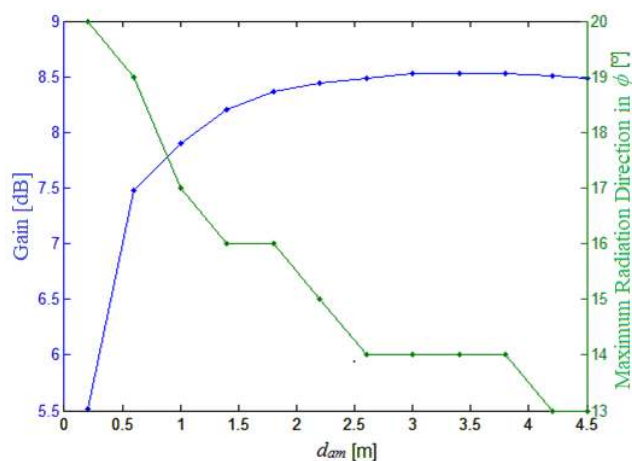


Fig. 8. Maximum gain and direction of maximum radiation vs.  $d_{am}$  for simulation T1.

### B. Simulations T5 and T6

Fig. 9 compares the reflection coefficient responses obtained in simulations T4 (one antenna) and T6 (two antennas), both in scenarios without the mast, for both antenna lengths. As it can be noticed, as the antennas gets closer to each other, the reflection coefficient is degraded and the resonance frequency increases. Fig. 10, on the other hand, presents the transmission coefficient responses obtained in simulations T5 (with mast) and T6 (without mast), for both antenna lengths. As it can be seen,  $S_{21}$  is the greatest at the resonance frequency, meaning that the coupling is the highest there. Also, the presence of the mast does not significantly affect the  $S_{21}$  responses.

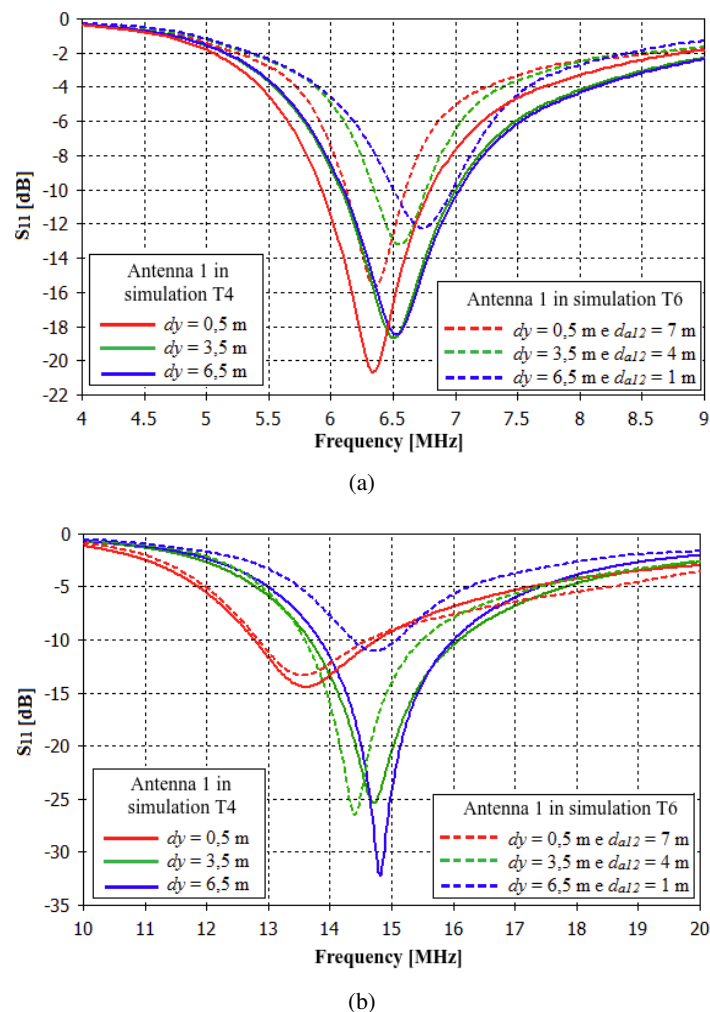


Fig. 9. Reflection coefficient for simulations T4 and T6. a) Antenna with  $\lambda = 44$  m, b) Antenna with  $\lambda = 20$  m.

Regarding the radiation pattern, in the  $\phi = 0^\circ$  plane, without the mast, the maximum gain of the two antennas increases as they are closer, and the lobe in  $\phi = 180^\circ$  is 1.2 dB greater than the lobe in the opposite direction. It is also worth mentioning that the null in  $\theta = 0^\circ$  seen for the reference antenna does not occur when there is another antenna in its vicinity. The gain in this direction decreases as the antennas get closer to each other. When considering the mast in the scenario, the most significant change is in the main lobe, which points to  $\phi = 0^\circ$  for  $d_{a12} \leq 1$  m, for both antennas, and both antenna lengths.

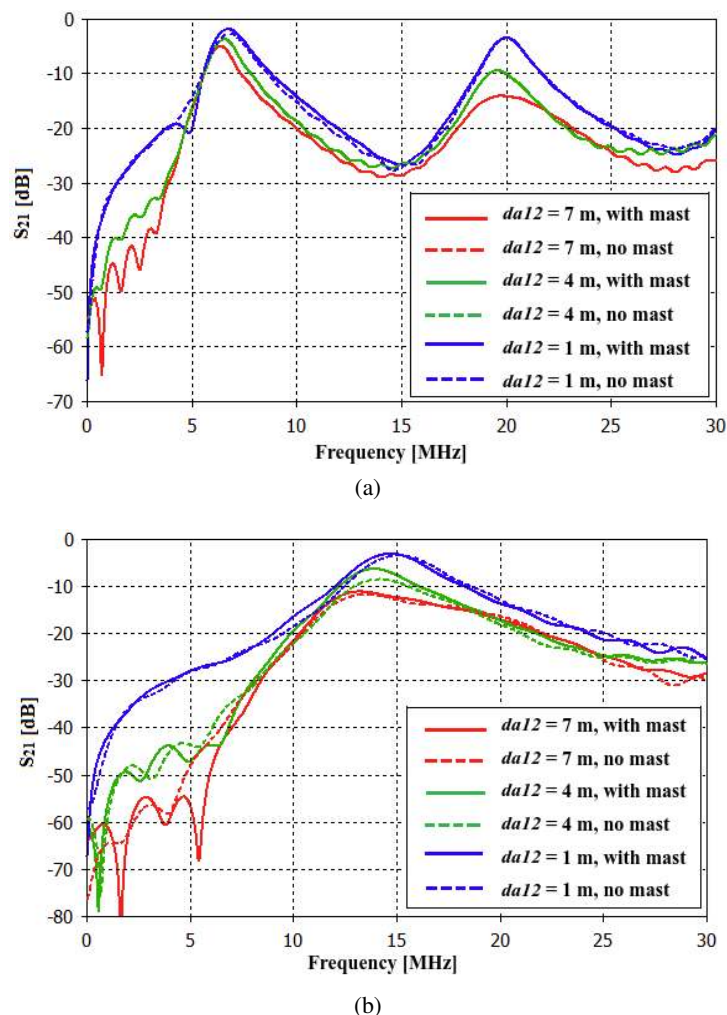


Fig. 10. Transmission coefficient for simulations T5 and T6. a) Antenna with  $\lambda = 44$  m, b) Antenna with  $\lambda = 20$  m.

For the  $\phi = 90^\circ$  plane, without considering the mast, the maximum gain of both antennas is practically constant for  $d_{a12} \geq 2$  m, and for shorter distances, it is decreased as well. For antenna 1, the lobe at  $\phi = 90^\circ$  is greater than the lobe in the opposite direction, and for  $d_{a12} \leq 0.1$  m, the main lobe changes the orientation. Antenna 2 behaves conversely, and the change of lobe direction takes place for  $d_{a12} \geq 7$  m. When considering the mast, the most significant change is in the main lobe, which points to  $\phi = 270^\circ$  for  $d_{a12} \leq 1$  m, for both antennas, and both antenna lengths.

Finally, in the  $\theta = 90^\circ$  plane, without the mast, the expected round shape of the gain pattern is lost for both antennas, and both antenna lengths. Regarding the angle of maximum radiation, for antenna 1, it increases as the two antennas are closer to each other. For antenna 2, this angle is practically constant for  $d_{a12} \geq 2$  m, and for smaller distances, it decreases. When considering the mast, for antennas 1 and 2, the most significant change occurs in the gain value. Moreover, in the maximum radiation angle for  $d_{a12} \leq 1$  m, it is noted that the two antennas have similar patterns, mirrored horizontally, for both antenna lengths.

### C. Decorrelation distances

After assessing the performance of the main figures of merit in the previous simulations, it was also possible to estimate some decorrelation distances between the monopoles and nearby objects, in order to aid the antenna positioning task in similar upper bridge scenarios. Thus, it is recommended that  $d_{am} \geq 3$  m, along the  $x$ -axis, and  $d_y \geq 6$  m. And when there are two antennas at the same side of the mast and parallel to each other, it is advised that  $d_{a12} \geq 4$  m.

## V. CONCLUSIONS

This work presented a parametric analysis on the positioning of HF monopole antennas on the upper bridge of a typical Navy frigate. The analysis was performed based on numerical simulations of a simplified model of that scenario in CST, considering essentially the effects of the main mast and the finite length and width of the upper bridge, besides the antennas. In order to assess the expected effects, figures of merit such as reflection coefficient and gain were calculated in all simulations, as well as the transmission coefficient between a pair of monopoles, when pertinent. The ideal monopole of infinite PEC ground plane was taken as a reference case in the analysis.

In general, based on the simulations without the mast, it was possible to observe that, when the antenna gets close to the edge, there is a slight decrease in the resonance frequency in comparison to the reference case, and a reduction of the minimum value of the reflection coefficient. Also, there is an increase in the input resistance and reactance. As for the gain pattern behavior, the main lobe direction changes, both in the  $\phi = 0$  and  $90^\circ$  planes, and the gain increases in the direction  $\theta = 0^\circ$ .

With the mast, as the antenna gets farther from the mast, the resonance frequency slightly decreases compared to the reference, the reflection coefficient improves considerably, and the input resistance and reactance variations increase. Regarding the radiation performance, the direction of the main lobe in the  $\phi = 0$  and  $90^\circ$  planes changes, and the pattern in the  $\theta = 90^\circ$  plane becomes directive. The mast does not affect much the mutual coupling between a pair of monopoles at the same side of the mast.

At last, from the obtained results, it was possible to estimate and recommend a few decorrelation distances between the monopoles and nearby objects in order to help the task of positioning the HF antennas on a typical frigate upper bridge. Provided the antenna is positioned in compliance with those distances, the coupling effects may be practically disregarded in the present scenario.

## ACKNOWLEDGMENTS

The authors would like to thank Diretoria de Comunicações e Tecnologia da Informação da Marinha (DCTIM) for the use of the numerical simulation tool chosen for this work.

## REFERENCES

- [1] D. G. Baker, *Electromagnetic Compatibility: Analysis and Case Studies in Transportation*. John Wiley & Sons, 2015.
- [2] L. G. da Silva *et al.*, "Electromagnetic characterization of aircraft composite materials and its effects on the antenna performance," *Journal of Microwaves, Optoelectronics and Electromagnetic Applications*, vol. 16, no. 1, pp. 218–236, 2017.
- [3] M. H. C. Dias, A. C. Silveira, and M. B. T. Dantas, "Análise da sintonia de uma antena monopolo HF em viatura tática de comando e controle (in Portuguese)," in *Anais do XXXVI Simpósio Brasileiro de Telecomunicações e Processamento de Sinais*, pp. 85–89, 2018.
- [4] F. C. S. Assumpção, A. C. Silveira, and M. H. C. Dias, "Análise da antena monopolo de quarto de onda encurvada (in Portuguese)," in *Anais do XXXVII Simpósio Brasileiro de Telecomunicações e Processamento de Sinais*, pp. 1–5, 2018.

- [5] M. Ignatenko and D. S. Filipovic, "Application of characteristic mode analysis to HF low profile vehicular antennas," in *2014 IEEE Antennas and Propagation Society International Symposium (APSURSI)*, pp. 850–851, 2014.
- [6] S. Sanghai, M. Ignatenko, and D. S. Filipovic, "Two arm offset fed inverted-L antenna for vehicular HF communications," in *2015 IEEE International Symposium on Antennas and Propagation & USNC/URSI National Radio Science Meeting*, pp. 1604–1605, 2015.
- [7] B. Allen, M. Ignatenko, and D. S. Filipovic, "Low profile vehicular antenna for wideband high frequency communications," in *2016 IEEE International Symposium on Antennas and Propagation Symposium (APSURSI)*, pp. 115–116, 2016.
- [8] R. A. Burberry, *VHF and UHF Antennas*. Institution of Electrical Engineers, 1992.
- [9] L. F. S. Alvarez and F. J. C. Dopazo, "Human exposure to electromagnetic fields on marine platforms: safety regulations, simulation and measurement," *IEEE Latin America Transactions*, vol. 16, no. 1, pp. 46–51, 2018.
- [10] International Electrotechnical Commission, *CISPR 25: Limits and methods of measurement of radio disturbance characteristics for protection of receivers used on board vehicles*. IEC, 2008.
- [11] G. Marrocco and L. Mattioni, "Naval structural antenna systems for broadband HF communications," *IEEE Transactions on Antennas and Propagation*, vol. 54, no. 4, pp. 1065–1073, 2006.
- [12] G. Marrocco, L. Mattioni, and V. Martorelli, "Naval structural antenna systems for broadband HF communications—part II: design methodology for real naval platforms," *IEEE Transactions on Antennas and Propagation*, vol. 54, no. 11, pp. 3330–3337, 2006.
- [13] L. Mattioni, D. Di Lanzo, and G. Marrocco, "Naval structural antenna systems for broadband HF communications—part III: experimental evaluation on scaled prototypes," *IEEE Transactions on Antennas and Propagation*, vol. 56, no. 7, pp. 1882–1887, 2008.
- [14] S. R. Best, "On the use of scale brass models in HF shipboard communication antenna design," *IEEE Antennas and Propagation Magazine*, vol. 44, no. 2, pp. 12–23, 2002.
- [15] T. Jagannath, P. Kulkarni, and V. Tyagi, "HF broadband antenna design considerations on warships," in *Proceedings of the International Conference on Electromagnetic Interference and Compatibility*, pp. 421–428, 1999.
- [16] Y. Chen and C.-F. Wang, "HF band shipboard antenna design using characteristic modes," *IEEE Transactions on Antennas and Propagation*, vol. 63, no. 3, pp. 1004–1013, 2015.
- [17] F. C. S. Assumpção and M. H. C. Dias, "Análise do posicionamento de antenas monopolo HF sobre o tijupá de uma fragata (in Portuguese)," in *Anais do MOMAG 2020/14° CBMag e 19° SBMO*, pp. 149–153, 2020.
- [18] B. Turetken, F. Ustuner, E. Demirel, and A. Dagdeviren, "EMI/EMC analysis of shipboard HF antenna by moment method," in *International Conference on Mathematical Methods in Electromagnetic Theory*, pp. 350–352, 2006.
- [19] M. M. Weiner, *Monopole antennas*. CRC Press, 2003.
- [20] C. A. Balanis, *Antenna theory: analysis and design*, 4th ed. John Wiley & Sons, 2016.
- [21] "CST Studio Suite 3D EM simulation and analysis software," Dassault Systèmes, accessed: 25 jan. 2021. [Online]. Available: <https://www.3ds.com/products-services/simulia/products/cst-studio-suite/>
- [22] F. C. S. Assumpção, "Análise eletromagnética do posicionamento de antenas de radiocomunicações em navios de marinha (in Portuguese)," Master's thesis, IME, Rio de Janeiro, 2020.